Effect of IC50 dose of retinol on metabolomics of RAW264.7 cells

Yali Wang
Shandong Normal University
Xiao Song
Shandong Normal University
Yue Geng (gengy@sdnu.edu.cn)
Shandong Normal Universuity

Research

Keywords: Retinol, RAW264.7, IC50, metabolomics, nuclear magnetic resonance

Posted Date: December 12th, 2019

DOI: https://doi.org/10.21203/rs.2.18678/v1

Abstract

Background: Vitamin A is one of the most multifunctional Vitamin in the human body and is involved in several basic physiological processes from embryonic development to adulthood, such as embryogenesis, vision, immunity, cell differentiation, and proliferation. The aim of current study was to identify its effects on the differential metabolites and main metabolic pathways. We also analyzed the toxicity of retinol.

Methods: In this study, we conducted proton nuclear magnetic resonance (NMR) to evaluate metabolomic changes in RAW264.7 cells after treatment with retinol at a half maximal inhibitory concentration (IC 50).

Results: Our results showed that the IC 50 dose (140 μM) of retinol affected the metabolism of RAW264.7 cells, with a total of 22 differential metabolites identified via 1 H-NMR, including amino acids, sugars, organic acids, glutathione, glycerin, and creatine. Additionally, multiple metabolic pathways were affected by retinol treatment, including amino acid biosynthesis, protein synthesis, and pyruvate metabolism. We speculate that the cytotoxicity of retinol at the IC 50 dose is attributed to mitochondrial dysfunction as a result of oxidative stress or lipid peroxidation.

Conclusions: RAW264.7 cells showed significant changes in protein biosynthesis, urea cycle, arginine and proline metabolism, malate-aspartate shuttle, alanine metabolism, and cellular respiration after treatment with retinol at the IC 50 dose (140 μM), indicating that retinol affects cellular physiological functions via different metabolic pathways.

1. Introduction

Vitamin A is a generic term for a group of fat-soluble, unsaturated organic compounds that includes retinol, retinal, and retinoic acid, among others [1]. Vitamin A and its precursors are mainly derived from livers, cod liver oil, dairy products, egg yolks, dark green leafy vegetables, dark yellow and orange vegetables and fruits, and vitamin supplements [2]. Vitamin A has various functions in the human body, such as maintaining normal vision and health of epithelial cells, promoting the synthesis of immunoglobulins, participating in the synthesis of glycoproteins [3], maintaining the normal growth and development of bones, and promoting protein biosynthesis and osteoblast differentiation [4]. The circulating form of vitamin A in the blood is retinol. After cellular uptake, retinol is converted into retinoic acid (RA), an active metabolite used by the immune system [5]. Both insufficient intake (which causes hypovitaminosis A) and excess intake (which causes hypervitaminosis A or vitamin A toxicity) of vitamin A can threaten human health [6]. Food fortification and dietary supplementation with retinyl ester are commonly employed to alleviate hypovitaminosis A. According to data from the World Health Organization (WHO), the Recommended Nutrient Intakes (RNIs) and Tolerable Upper Intake Level (UL) of vitamin A for a healthy adult males are 1998 IU and 9990 IU, respectively [7]. However, because of the rising interest in fortified foods and vitamin A supplements, most healthy individuals exceed the recommended dose of vitamin A [8].

Numerous studies have shown that excessive vitamin A intake may lead to neurological side effects [9], osteoporosis and fractures [10], and various structural abnormalities during embryogenesis [11, 12]. Yeh et al. suggested that vitamin A overdose (25,000–50,000 IU) can lead to liver damage and renal insufficiency in rats, and the mechanism underlying liver damage may be attributed to lipid peroxidation [13]. A study by Schuster et al. revealed that a high level of vitamin A (250 IU/g in diets) resulted in severe excessive airway inflammation and airway hyperresponsiveness by enhancing serum IgE and IgG1 responses and pulmonary eosinophilic inflammation in mice. Additionally, a high level of vitamin A shifts the Th1/Th2 balance towards Th2, leading to the aggravation of experimental asthma [14]. Bray et al. confirmed that retinol (75 mg/kg·day) significantly decreased the enzymatic activity and polypeptide levels of CYP3A in the liver and exacerbated the acetaminophen-induced liver toxicity [15]. High doses of vitamin A (1700 IU/g) directly reduced the bone diameter in rats and indirectly affected serum biomarkers of bone length, turnover, mineral density, and cortical bone [16]. A previous study demonstrated the involvement of the Wnt5a/CaMKII pathway in retinoic acid (RA)-induced developmental abnormalities in mouse genioglossus [17]. Retinoic acid (10 μM) inhibits the proliferation and differentiation of C2C12 cells by upregulating the expression of miR-31-5p and miR-27b-3p and downregulating the expression of CamkIIδ and DTNA [18, 19]. Exogenous RA (3 μM) promotes the apoptosis and inhibits the proliferation of epithelial cells lining the labial cervical loop by downregulating the expression of the mesenchymal factor Fgf10, thereby negatively regulating the homeostasis of the incisor stem cell niche. These effects are accompanied by inhibition of Bcl2 expression [20]. Zhang et al. suggested that all-trans retinoic acid (200 mg/kg) induces cleft palate by inhibiting degradation of the medial edge epithelium via the Notch1/RBPjk/P21 signaling pathway [21]. Liu et al. showed that excessive RA (100 mg/kg) induced cleft palate by downregulating the expression of histone methyltransferase in palate mesenchymal cells [22]. It has also been shown that RA-induced cleft palate is also attributable to downregulation of the classical Wnt/β-catenin signaling pathway [23]. Zhang et al. showed that all-trans retinoic acid (1 μM) inhibited cartilage-specific molecules (including aggrecan, Sox9, and Col2al) by regulating the expression of p53 and p21 to reduce chondrogenesis in rat embryo hindlimb bud mesenchymal cells, thereby inducing the onset of congenital club foot [24].

Metabolomics is an emerging field that can determine changes in gene expression levels by detecting changes in metabolite levels via metabolomics techniques, thereby indicating the functions of genes and their effects on metabolic flux. Metabolomics not only allows for the comprehensive analyses of individual metabolites, but also increases the understanding of metabolic pathways and various complex interactions in organisms, as well as responses of biological systems to environmental and genetic changes [25]. Currently, most studies on vitamin A have been based on genomics, transcriptomics, and proteomics; very few studies have examined its metabolomic aspects. Additionally, most studies evaluated the metabolic pathways of endogenous vitamin A [26, 27], while the toxicity of exogenous vitamin A has rarely been reported. Therefore, we evaluated the effects of vitamin A (retinol) at the IC_{50} dose on the metabolomics of RAW264.7 cells via metabolomic techniques to investigate changes in metabolite levels in normal cells treated with retinol at an IC_{50} dose to provide a theoretical basis for studying the toxicity of retinol.

2. Materials And Methods

2.1 Reagents and Instruments.

RAW264.7 cells were purchased from the Chinese Type Culture Collection (CTCC, Shanghai, China).

The following reagents were used: retinol (purity ≥ 95%, 17772) and D_2O containing 0.1% TSP (Sigma-Aldrich, St. Louis, MO, USA); DMEM culture medium (HyClone, Logan, UT, USA); dimethyl sulfoxide, and MTT (Solarbio, Beijing, China); penicillin, streptomycin, and L-glutamine (M&C Gene Technology Ltd., Beijing, China); fetal calf serum (Zhejiang Tianhang Biotechnology Co., Ltd., Hangzhou, China); and mouse interleukin (IL)-1β ELISA kit, mouse IL-6 ELISA kit, and mouse tumor necrosis factor (TNF)-α ELISA kit (Multi Sciences, Hangzhou, China).

The following instruments were used: Stat Fax-2000 Microplate Reader (Awareness Technology, Palm City, FL, USA); Epsilon 2–4 LSCplus freeze-dryer (Christ, Osterode, Germany); Centrifuge 5804R (Eppendorf, Hamburg, Germany); SB-1000 (Eyela, Tokyo, Japan); VC 130 PB (Sonic Materials, Inc., Newtown, CT, USA); AVANCE III 600 MHz (Bruker Biospin, Zurich, Switzerland); LabServ CO_2 incubator (Thermo Fisher Scientific, Waltham, MA, USA).

2.2 Solution Preparation

Retinol was dissolved in ethanol solution to prepare a stock solution with a gradient concentration and stored at -80 °C. Next, the stock solution was diluted to the required concentrations (80, 100, 120, 140, 160, 180 μM) with basic medium to ensure a final volume fraction of ethanol of 0.5%. The solutions were filtered and sterilized with a 0.22-μm microfiltration membrane and then protected from light.

2.3 Cell Culture

RAW264.7 cells were incubated in DMEM supplemented with 100 U/mL of penicillin, 100 μg/mL of streptomycin, 10 μg/mL of L-glutamine, and 10% fetal bovine serum. This cell line was originated from macrophages from ascites in the leukemia virus-induced tumor Abelson murine. The cells were cultured at 37 °C at 5% CO_2 and 95% humidity.

2.4 Cell Viability Assay

To test the effects of retinol on cell viability, an MTT assay was conducted. Cells in suspension were added to 96-well plates at 1×10^5 cells/well and incubated for 24 h at 37 °C. After removing the culture medium, fresh culture medium containing different concentrations of retinol (80, 100,120, 140, 160, and 180 μM) was added. The cells were incubated for 24 h at 37 °C. Next, 20 μL of MTT was added to each well and the plate was incubated for 4 h at 37 °C. The culture medium in each well was removed, and 150

μL/well of dimethyl sulfoxide was added followed by incubation for 20 min with shaking at room temperature. The absorbance of the cell suspension was measured at 492 nm with a microplate reader.

2.5 Cytokine Assay

The IC_{50} value of retinol in RAW264.7 cells was determined from the MTT assay results. Cells in suspension were placed in 24-well plates at 1×10^6 cells/well and incubated for 12 h at 37 °C. After the cells were attached, the original medium was discarded and the IC_{50} dose of retinol group was added (RET group); non-treated cells were used as control (Control group). After 24 h, the culture medium was removed and centrifuged at 3000 rpm for 10 min. The supernatant was stored at -20 °C. IL-1β, IL-6, and TNF-α were quantified by using mouse ELISA kits (3 parallel groups were used for each experimental group).

2.6 ^{1}H-NMR

2.6.1 Cell Extraction

After the cells were treated with retinol at the IC_{50} concentration for 24 h at 37 °C, the original culture solution was discarded, the cells were washed with PBS three times, and 4 mL of cold methanol was added to quench the cells. The cells were removed from the culture dishes with a cell scraper, suspended in ice-cold methanol, and stored at − 4 °C. The cell suspensions in methanol were then mixed with ultrapure water and trichloromethane at a ratio of 2.85:4:4 (V:V:V, ultrapure water: methanol: trichloromethane). After vortexing, the cell suspensions were sonicated to break up cells. Sonication was performed in an ice water bath with 1-min sonication/break alternations for a total of 9 min. The aqueous phase was separated from the organic phase by centrifugation at 12,000 rpm and 4 °C for 30 min. After centrifugation, the clear aqueous supernatant was collected. The same extraction process was repeated three times. The supernatant liquid was combined and stored at − 80 °C. The aqueous supernatant samples were evaporated at 60 °C, and the solid compound was dissolved in 900 μL of D_2O (pH 7.4, containing 0.1% TSP). The 12 samples were centrifuged at 12,000 rpm and 4 °C for 15 min and lyophilized. The lyophilized samples were re-dissolved in 700 μL of D_2O and centrifuged under the same conditions described above. From the aqueous supernatant, 600 μL was mixed with 50 μL of phosphate buffer solution containing D_2O (pH 7.4, containing 0.1% TSP). The supernatant (550 μL) was collected into a 5-mm NMR tube for analysis.

2.6.2 ^{1}H-NMR Spectroscopy Analysis

All ^{1}H-NMR spectra were obtained with a superconductor shielding Fourier transform NMR spectrometer equipped with ^{13}C and ^{1}H double resonance optimization of a 5-mm CPTCI three trans detector

CryoProbeTM AVANCE 600 III (Bruker) under the following conditions: 600.104 MHz for proton resonance frequency, zg30 for pulse sequence, 12,019.230 Hz for spectral width, 16 repetitions, 2 dummy scans at 298 K, 1-s relaxation delay, and 12-μs pulse length. Topspin 3.2 was used to process the spectral data.

2.7 Data Analysis

2.7.1 Data Analysis for ^{1}H-NMR Spectroscopy

The NMR spectra were processed with MestReNova 6.11 (Mestrelab Research, Santiago de Compostela, Spain). For all spectra, the exponential window function was added and processing was conducted with manual baseline correction. Using TSP as the standard, the spectra were manually cut off from the water peak and normalized. Data for the integrated peak were exported into numbered groups in Excel files. Next, the data were imported into SIMCA-P 14.1 software (Umetrics, Inc., Umea, Sweden). The data were analyzed using principal component analysis, partial least-squares-discriminant analysis (PLS-DA), and orthogonal partial least-squares-discriminant analysis (OPLS-DA). The reliability of the PLS and OPLS-DA models was verified by permutation testing and CV-analysis of variance.

Differential metabolites were identified based on variable importance in projection (VIP) and loading weights of the primary predictive component. The chemical shifts (δ) were selected with the standard of their values of VIP ≥ 1. Next, the values of chemical shift were imported into the Biological Magnetic Resonance Bank, and a list of possible materials was compiled. Based on the list, we identified substances matching the locations and patterns of peaks in the human metabolome database. To quantify the up- and downregulation of metabolites, we normalized the peak areas of identified the metabolites by summing the metabolites of the integral area multiplied by 1000 (relative value).

After identifying certain metabolites, we enriched the pathways using the Kyoto Encyclopedia of Genes and Genomes (KEGG) and MetaboAnalyst (MetPA). The metabolites were imported into KEGG to obtain a list of their KEGG ID numbers. Next, the list was imported into MetPA to match the metabolic pathways using two methods. In pathway analysis, pathway impact characterization was used to draw graphs with the topology based on the importance of the metabolic pathways using the computed value, while the ordinated − log P revealed significant metabolic pathways in enrichment analysis. Another method for analyzing the functional enrichment analysis of humans and mammals is metabolite set enrichment analysis. We conducted overrepresentation analysis a list of compound names was provided.

2.7.2 Statistical Analysis

Statistical analysis was performed using paired Student's t test or multi-way analysis of variance. Statistical analysis was conducted using Graphpad Prism software (GraphPad, Inc., La Jolla, CA, USA). Differences were considered as statistically significant when $p < 0.05$. All experiments were conducted independently at least three times.

3. Results

3.1 Effects of Retinol (RET) on RAW264.7 Cell Viability

The results of the MTT assay revealed significant inhibition of cell viability after treatment with retinol for 24 h. According to the regression equation, the IC_{50} of retinol for RAW264.7 cells was 138.69 μM (see Fig. 1), which was rounded to 140 μM for subsequent experiments.

3.2 Effects of RET on Cytokine Secretion in RAW264.7 Cells

Figure 2a shows that both the retinol and control group had similar levels of the IL-1β, suggesting that retinol does not significantly affect the level of IL-1β secreted from RAW264.7 cells. Figure 2b and 2c show that the concentrations of IL-6 and TNF-α secreted from retinol-treated cells were elevated by approximately 6- and 5-fold, respectively ($p < 0.005$), indicating that retinol treatment significantly enhanced the secretion of IL-6 and TNF-α from RAW264.7 cells.

3.3 Analysis of ^{1}H-NMR Results

3.3.1 Analysis of ^{1}H-NMR Spectra

Figure 3a shows the one-dimensional ^{1}H NMR spectra of RAW264.7 cells from the retinol and control groups, respectively. The chemical shifts represent different compounds, while the signal intensity represents the concentration of the respective chemical substances. There were significant differences in the types and concentrations of metabolites between the retinol group and control group, suggesting that cellular metabolites are affected and altered by retinol treatment at the IC_{50} dose.

3.3.2 Multivariate Statistical Analysis

The integrated areas under the chemical shifts derived from the NMR spectra were imported in an Excel format into SIMCA-P14.1 software for multivariate statistical analysis.

Figure 3b shows the PCA score plots of RAW264.7 cells. The retinol group and control group significantly differed based on the first and second principal components. To achieve more accurate grouping, we used supervised analytical methods, such as PLS-DA and OPLS-DA, for data processing. Figures 3c and 3d show the PLS-DA and OPLS-DA score plots of RAW264.7 cells. The results showed that the retinol group and the control group significantly differed based on the first and second principal components with clear separations, indicating altered metabolite production in retinol-treated cells. We employed the permutation test to examine these models to evaluate their reliability. Figures 3e and 3f show the results for the PLS-DA and OPLS-DA models for RAW264.7 cells. The random R^2 and Q^2 values were lower than the rightmost point in both models. Furthermore, $R^2 > 0$, $Q^2 < 0$, and the rightmost values of the regression equation of R^2 and Q^2 were close to 1, suggesting that these

models were not overfitted and are reliable.

In summary, the retinol group (RAW264.7 cells treated with retinol at the IC_{50} concentration) and control group differed and were significantly distinguishable from one another.

3.3.3 Qualitative and Metabolic Pathway Analyses of Differential Metabolites

We ranked the VIP values from multivariate statistical analyses in descending order to identify the differential metabolites. Because of the large number of substances with VIP ≥ 1, chemical shifts with VIP ≥ 2 were used to quantitatively analyze the metabolites. The confirmed differential metabolites are listed in Table 1. A total of 22 differential metabolites, including amino acids, sugars, organic acids, glutathione, glycerin, and creatine, were identified.

Table 1
Differential metabolites in RAW264.7 cell line.

No.	Metabolites	δ(ppm)	multiplicity	Matching shifts	VIP	Trend
1	Argininosuccinic acid	3.27	t	66	11.31	↓
2	L-Glutamine	2.446	m	56	3.75	↓
3	L-Glutamic acid	2.341	m	56	4.56	↓
4	Glutathione	2.54	m	49	2.95	↓
5	L-Homoserine	2.01	m	44	6.76	↓
6	2-amino-3-phosphonopropionic	3.81	dd	44	6.24	↓
7	Linoleic acid	2.06	m	39	3.34	↓
8	D-xylose	3.42	t	36	7.13	↑
9	L-Aspartic acid	2.80	dd	33	4.60	↓
10	Shikimic acid	4.01	m	30	2.11	↓
11	L-Alanine	3.76	q	29	7.04	↓
12	L-Malic acid	2.66	dd	29	7.38	↓
13	Allose	3.87	dd	25	3.25	↓
14	Fructose-6-phosphate	3.65	m	25	5.38	↑
15	1-Methyhistidine	3.68	s	24	4.95	↑
16	Glycerol	3.551	m	23	4.66	↓
17	Pipecolic acid	2.99	td	22	2.68	↓
18	Malic acid	2.66	dd	22	4.93	↓
19	Homocysteine	2.14	m	21	3.88	↓
20	L-Proline	4.12	dd	21	4.68	↓
21	Betaine	3.25	s	20	4.02	↑
22	Creatine	3.02	s	20	3.87	↑

To study the metabolic pathways of biomarkers associated with retinol treatment in RAW264.7 cells, we explored their potential interactions using the KEGG database. We further confirmed the effects of retinol on these metabolic pathways using MetPA (Fig. 4). The 22 differential metabolites were mapped to a total of 24 metabolic pathways, such as the metabolism of various amino acids (including arginine and proline), citric acid cycle, metabolism of various organic acids (such as pyruvic acid), carbohydrate

metabolism, lipid metabolism, nitrogen metabolism, and biosynthesis of unsaturated fatty acids (Table 2). Subsequent metabolite set enrichment analysis revealed changes in multiple metabolic pathways, including 29 metabolic pathways with different degrees of inhibition: biosynthesis of proteins; urea cycle; metabolism of arginine and proline; malate-aspartate shuttle; metabolism of alanine; ammonia recycling; metabolism of methionine; metabolism of betaine; metabolism of glycine, serine, and threonine; metabolism of histidine; metabolism of aspartic acid; glucose-alanine cycle; metabolism of β-amino alanine; metabolism of glutamate; gluconeogenesis; metabolism of cysteine; metabolism of alpha-linolenic acid and linoleic acid; metabolism of glutathione; metabolism of pyrimidine; metabolism of glycerides; metabolism of selenium amino acids; metabolism of amino sugars; pentose phosphate pathway; degradation of fructose and mannose; metabolism of pyruvic acid; glycolysis; citric acid cycle; metabolism of galactose; and metabolism of purine.

Table 2

Metabolic pathways belonging to differential metabolites in RAW264.7 cell line

NO.	Pathway	Total	Expected	Hits	Holm adjust	Impact
1	Alanine, aspartate and glutamate metabolism	24	0.33874	5	0.000965	0.62447
2	Arginine and proline metabolism	44	0.62103	6	0.001436	0.19309
3	Histidine metabolism	15	0.21171	3	0.078664	0
4	D-Glutamine and D-glutamate metabolism	5	0.070572	2	0.14584	1
5	Aminoacyl-tRNA biosynthesis	69	0.97389	5	0.16175	0
6	Nitrogen metabolism	9	0.12703	2	0.49465	0
7	Glycine, serine and threonine metabolism	31	0.43754	2	1	0
8	Linoleic acid metabolism	6	0.084686	1	1	1
9	Selenoamino acid metabolism	15	0.21171	1	1	0
10	Pentose and glucuronate interconversions	16	0.22583	1	1	0.13333
11	beta-Alanine metabolism	17	0.23994	1	1	0
12	Glyoxylate and dicarboxylate metabolism	18	0.25406	1	1	0
13	Glycerolipid metabolism	18	0.25406	1	1	0.28098
14	Citrate cycle (TCA cycle)	20	0.28229	1	1	0.0452
15	Butanoate metabolism	22	0.31052	1	1	0
16	Lysine degradation	23	0.32463	1	1	0
17	Pyruvate metabolism	23	0.32463	1	1	0
18	Galactose metabolism	26	0.36697	1	1	0
19	Glutathione metabolism	26	0.36697	1	1	0.05534
20	Porphyrin and chlorophyll metabolism	27	0.38109	1	1	0
21	Amino sugar and nucleotide sugar metabolism	37	0.52223	1	1	0
22	Pyrimidine metabolism	41	0.57869	1	1	0
23	Biosynthesis of unsaturated fatty acids	42	0.5928	1	1	0

NO.	Pathway	Total	Expected	Hits	Holm adjust	Impact
24	Purine metabolism	68	0.95977	1	1	0

4. Discussion

Macrophages are monocyte-derived leukocytes present in tissues and play important roles in host defense, tissue development, and homeostasis [28]. The mouse macrophage cell line RAW264.7 is derived from peritoneal effusion of male Balb/c mice. These immune cells are commonly used for laboratory experiments because of their high adhesive and phagocytic capacities [29]. Numerous studies have evaluated the mechanism of macrophage activation using metabolomic techniques. For example, Wu et al. studied the anti-inflammatory effect of non-steroidal anti-inflammatory drugs on RAW264.7 cells through the ultra-high-performance liquid chromatography/quadrupole time-of-flight mass spectrometry method and found that the effects were related to changes in glycerophospholipid metabolism [30]. Aarash et al. conducted gas chromatography-mass spectrometry and suggested that lipopolysaccharide activates macrophages by downregulating the de novo synthesis of nucleotides, which is regulated by the glutamate-glutamine complex and the malate-aspartate shuttle [31].

Our results showed that retinol significantly increased the levels of IL-6 and TNF-α in RAW264.7 cells but did not affect IL-1β levels. Several studies have demonstrated the effects of vitamin A on cytokines. Retinoic acid increased the transcription levels of IL-6 (by upregulating the transcription and stability of mature transcripts), monocyte chemoattractant protein-1, granulocyte-macrophage colony-stimulating factor, and IL-10 in macrophages [32]. Treatment of Wistar rats with vitamin A (2500 IU/kg·day) for 3 months enhanced monoamine oxidase activity, mitochondrial redox dysfunction, and TNF-α levels [33]. Gasparotto et al. found that vitamin A (2000 IU/kg, oral) reduced the pulmonary levels of superoxide dismutase, increased the levels of lipid peroxidation and protein carbonylation, and increased the level of TNF-α while decreasing the level of IL-10, but it did not affect the level of IL-1β in rats [34], which is consistent with our findings for cytokines.

Excessive retinol can enhance the production of free radicals and cause oxidative stress, thereby resulting in early apoptosis due to necrosis [35]. Different doses of vitamin A (1000, 2500, or 4500 IU/kg) induced the onset of a pro-oxidation state and large-scale production of superoxide anions in the hippocampus of adult rats, leading to oxidative stress and hippocampal toxicity [36]. Vitamin A supplementation induced oxidative damage to biomolecules [37], upregulation of antioxidant enzymes [38, 39], and activation of phosphorylation signaling pathways in Sertoli cells [40–42]. These results strongly suggest that vitamin A promotes oxidative stress and has potential pro-oxidative capacity. In this study, we observed reduced glutathione levels and elevated betaine levels, both of which are differential metabolites in cells. Glutathione is a major redox “buffer” in the cytoplasm [43], while betaine is widely considered as an antioxidant that can alleviate oxidative stress [44] [45]. Therefore, we predicted that after treatment with retinol at the IC_{50}, the large amount of RET entering the cells could cause mitochondrial dysfunction and

lipid peroxidation to result in massive superoxide anion production because of the leakage of the electron transport chain, thereby leading to oxidative stress responses. The significantly elevated levels of IL-6 and TNF-α indicated that the onset of intracellular inflammatory responses may be attributed to the maintenance of steady-state mitochondrial activity in cells because of mitochondrial dysfunction [46].

We also found that RET significantly downregulated the levels of argininosuccinic acid and L-malic acid and significantly increased the levels of fructose-6-phosphate. Metabolic pathway mapping of differential metabolites revealed the participation of argininosuccinic acid in the metabolism of arginine and proline; metabolism of alanine, aspartic acid and glutamate and the participation of L-malic acid in the metabolism of glyoxylic acid and dicarboxylic and tricarboxylic acid (TCA) cycles as well as the metabolism of pyruvic acid (see Table 2). The results of pathway enrichment revealed varying degrees of abnormalities in the malate-aspartate shuttle, TCA cycle, and pyruvic acid metabolism, suggesting abnormalities in cellular energy metabolism that eventually led to cell death.

Argininosuccinic acid is a basic amino acid synthesized from citrulline and aspartic acid in some cells and is used as a precursor for arginine in the urea cycle and citrulline-NO cycle. Additionally, argininosuccinic acid is the precursor for fumaric acid in TCA cycle [47]. L-malic acid is another important metabolic intermediate of fumaric acid in the TCA cycle. Malic acid can be synthesized in the body through the TCA or Krebs cycle in the mitochondria, or can be formed from pyruvic acid as the anaplerotic reaction. Under aerobic conditions, it is well-known that malic acid serves a crucial role in energy generation in the body. Malic acid can be oxidized into oxaloacetate, providing the reducing equivalent in the mitochondria via the malate-aspartate redox shuttle [48, 49]. Wang et al. found that the concentrations of metabolic intermediates of the TCA cycle, i.e., oxalosuccinate, and precursor of fumaric acid, i.e., argininosuccinate, decreased during late pregnancy, indicating a reduced demand for the TCA cycle. Such changes may be attributed to reduced aerobic oxidation of glucose to ensure a sufficient glucose supply for fetal development during late pregnancy [50]. Our experimental results partially agree with the above findings. Therefore, we predicted that retinol caused abnormalities in the metabolism of pyruvic acid and the TCA cycle by significantly downregulating the levels of argininosuccinic acid and L-malic acid, leading to cellular energy abnormalities that reduced aerobic respiration in cells. Elevation of fructose-6-phosphate may be caused by the accumulation of anaerobic respiration-related molecules, suggesting a conversion from aerobic to anaerobic respiration that reduces the cellular energy supply. Previous analyses of retinol-induced mitochondrial dysfunction and electron transport chain leakage appear to support our hypothesis. Furthermore, the reduction of argininosuccinic acid can lead to urea cycle disorders, which are biochemically characterized by aggravated argininosuccinic acid and arginine deficiencies [51]. In humans, the urea cycle mainly occurs in the liver, and thus excessive retinol can lead to urea cycle abnormalities that cause hyperammonemia, leading to hepatotoxicity and neurotoxicity of the elevated creatine levels provide an basis for our prediction.

5. Conclusion

In conclusion, RAW264.7 cells showed significant changes in protein biosynthesis, urea cycle, arginine and proline metabolism, malate-aspartate shuttle, alanine metabolism, and cellular respiration after treatment with retinol at the IC_{50} dose (140 μM), indicating that retinol affects cellular physiological functions via different metabolic pathways. After treatment with the IC_{50} dose (140 μM) of retinol, the cells showed significantly increased levels of oxidative stress, IL-6, and TNF-α, likely because of the mitochondrial dysfunction and lipid peroxidation caused by retinol treatment. In this study, we investigated the adverse effects of high-dose retinol from a metabolomic perspective by evaluating changes in metabolites and metabolic pathways. However, the specific molecular mechanism underlying retinol-induced mitochondrial dysfunction remains unclear and requires further study.

Abbreviations

IC:a half maximal inhibitory concentration; NMR:nuclear magnetic resonance; RA:retinoic acid; WHO:world health organization; RNIs:recommended nutrient intakes; UL:tolerable upper intake level; DMSO:Dimethyl Sulphoxide; FBS:fetal calf serum; MTT:3-(4,5-dimethylthiazol-2-yl)-2,5-diphenyltetrazolium bromide; RET:retinol; PCA:principal components analysis; TPLS-DA:partial least squares-discriminant analysis; OPLS-DA:orthogonal partial least squares-discriminant analysis; VIP:variable importance in projection; HMDB:human metabolome database; BMRB:Biological Magnetic Resonance Bank; KEGG:Kyoto Encyclopedia of Genes and Genomes; MetPA:MetaboAnalyst; MSEA:metabolite set enrichment analysis; CA:tricarboxylic acid.

Declarations

Acknowledgement

We thank Editage Company for its linguistic assistance during the preparation of this manuscript.

Funding

Not applicable.

Author contributions

YW conceived, designed and performed research, analyzed data and wrote the first draft of the paper. XS performed research and reviewed the manuscript. YG conceived and designed the research, and reviewed the manuscript. All authors have read the manuscript before submission.

Availability of data and materials

The datasets used and analyzed during the current study are available from the corresponding author (YG) upon reasonable request.

Ethics approval and consent to participate

This study did not involve the use of animal or human samples.

Consent for publication

All the authors gave their consent to the publication. The work described was original research that has not been published previously, and is not under consideration for publication elsewhere, in whole or in part.

Competing interests

The authors declare that they do not have any conflict of interest.

Author details

Key Laboratory of Food Nutrition and Safety of SDNU, Provincial Key Laboratory of Animal Resistant Biology, College of Life Science, Shandong Normal University, Jinan 250014, China

References

1. Tanumihardjo SA, Russell RM, Stephensen CB et al. Biomarkers of Nutrition for Development (BOND)—Vitamin A Review. The Journal of Nutrition **2016**;146(9):1816S-1848S. https://doi.org/10.3945/jn.115.229708.
2. Dary O, Mora JO. Food fortification to reduce vitamin A deficiency: International Vitamin A Consultative Group recommendations. J NUTR **2002**;132(9):2927S-2933S. https://doi.org/10.1093/jn/132.9.2927S.
3. Kim YK, Wassef L, Chung S et al. beta-Carotene and its cleavage enzyme beta-carotene-15,15'-oxygenase (CMOI) affect retinoid metabolism in developing tissues. FASEB J **2011**;25(5):1641-1652. https://doi.org/10.1096/fj.10-175448.
4. Morris PJ, Salt C, Raila J et al. Safety evaluation of vitamin A in growing dogs. BRIT J NUTR **2012**;108(10):1800-1809. https://doi.org/10.1017/S0007114512000128.
5. D'Ambrosio DN, Clugston RD, Blaner WS. Vitamin A metabolism: an update. NUTRIENTS **2011**;3(1):63-103. https://doi.org/10.3390/nu3010063.
6. Li Y, Wongsiriroj N, Blaner WS. The multifaceted nature of retinoid transport and metabolism. Hepatobiliary Surgery and Nutrition 2014;3(3):126-139. https://doi.org/10.3978/j.issn.2304-3881.2014.05.04.
7. Allen, L., Dary, O., Benoist, B.D., Hurrell, R. Guidelines on food fortification with micronutrients. World Health Organization, France **2006**. https://doi.org/ 10.1108/13665620610647818.
8. Schnorr C, Morrone M, Simões-Pires A, Bittencourt L, Zeidán-Chuliá F, Moreira J. Supplementation of Adult Rats with Moderate Amounts of β-Carotene Modulates the Redox Status in Plasma without Exerting Pro-Oxidant Effects in the Brain: A Safer Alternative to Food Fortification with Vitamin A? Nutrients **2014**;6(12):5572. https://doi.org/10.3390/nu6125572.

9. Faustino JF, Ribeiro-Silva A, Dalto RF et al. Vitamin A and the eye: an old tale for modern times. Arquivos Brasileiros de Oftalmologia **2016**;79:56-61. http://doi.org/10.5935/0004-2749.20160018.
10. Saeed A, Dullaart RPF, Schreuder TCMA, Blokzijl H, Faber KN. Disturbed Vitamin A Metabolism in Non-Alcoholic Fatty Liver Disease (NAFLD). NUTRIENTS **2017**;10(1):29. https://doi.org/10.3390/nu10010029.
11. Wassef L, Shete V, Costabile B, Rodas R, Quadro L. High Preformed Vitamin A Intake during Pregnancy Prevents Embryonic Accumulation of Intact β-Carotene from the Maternal Circulation in Mice. The Journal of Nutrition **2015**;145(7):1408-1414. https://doi.org/10.3945/jn.114.207043.
12. Piersma AH, Hessel EV, Staal YC. Retinoic acid in developmental toxicology: Teratogen, morphogen and biomarker. REPROD TOXICOL **2017**;72:53-61. https://doi.org/10.1016/j.reprotox.2017.05.014.
13. Yeh Y, Lee Y, Hsieh Y. Effect of cholestin on toxicity of vitamin A in rats. FOOD CHEM **2012**;132(1):311-318. https://doi.org/10.1016/j.foodchem.2011.10.082.
14. Schuster GU, Kenyon NJ, Stephensen CB. Vitamin A Deficiency Decreases and High Dietary Vitamin A Increases Disease Severity in the Mouse Model of Asthma. The Journal of Immunology **2008**;180(3):1834. https://doi.org/10.4049/jimmunol.180.3.1834.
15. Bray BJ, Goodin MG, Inder RE, Rosengren RJ. The effect of retinol on hepatic and renal drug-metabolising enzymes. FOOD CHEM TOXICOL **2001**;39(1):1-9. https://doi.org/10.1016/S0278-6915(00)00110-1
16. Lind T, Lind PM, Hu L, Melhus H. Studies of indirect and direct effects of hypervitaminosis A on rat bone by comparing free access to food and pair-feeding. UPSALA J MED SCI **2018**;123(2):82-85. https://doi.org/10.1080/03009734.2018.1448020.
17. Cong W, Liu B, Liu S et al. Implications of the Wnt5a/CaMKII pathway in retinoic acid-induced myogenic tongue abnormalities of developing mice. SCI REP-UK **2014**;4:6082. https://doi.org/10.1038/srep06082.
18. Liu B, Liu C, Cong W et al. Retinoid acid-induced microRNA-31-5p suppresses myogenic proliferation and differentiation by targeting CamkIIδ. SKELET MUSCLE **2017**;7(1):8. https://doi.org/10.1186/s13395-017-0126-x.
19. Li N, Tang Y, Liu B, Cong W, Liu C, Xiao J. Retinoid acid-induced microRNA-27b-3p impairs C2C12 myoblast proliferation and differentiation by suppressing α-dystrobrevin. EXP CELL RES **2017**;350(2):301-311. https://doi.org/10.1016/j.yexcr.2016.11.009.
20. Xi J, He S, Wei C et al. Negative effects of retinoic acid on stem cell niche of mouse incisor. STEM CELL RES **2016**;17(3):489-497. https://doi.org/10.1016/j.scr.2016.09.030.
21. Zhang Y, Dong S, Wang W et al. Activation of Notch1 inhibits medial edge epithelium apoptosis in all-trans retinoic acid-induced cleft palate in mice. BIOCHEM BIOPH RES CO **2016**;477(3):322-328. https://doi.org/10.1016/j.bbrc.2016.06.107.
22. Liu S, Higashihori N, Yahiro K, Moriyama K. Retinoic acid inhibits histone methyltransferase Whsc1 during palatogenesis. BIOCHEM BIOPH RES CO **2015**;458(3):525-530. https://doi.org/10.1016/j.bbrc.2015.01.148.

23. Hu X, Gao J, Liao Y, Tang S, Lu F. Retinoic acid alters the proliferation and survival of the epithelium and mesenchyme and suppresses Wnt/β-catenin signaling in developing cleft palate. CELL DEATH DIS **2013**;4(10):e898. https://doi.org/10.1038/cddis.2013.424.
24. Zhang T, Li X, Yu G et al. All-trans-retinoic acid inhibits chondrogenesis of rat embryo hindlimb bud mesenchymal cells by downregulating p53 expression. MOL MED REP **2015**;12(1):210-218. https://doi.org/10.3892/mmr.2015.3423.
25. Liu X, Locasale JW. Metabolomics: A Primer. TRENDS BIOCHEM SCI **2017**;42(4):274-284. https://doi.org/10.1016/j.tibs.2017.01.004.
26. Wu J, Yang R, Zhang L et al. Metabolomics research on potential role for 9-cis-retinoic acid in breast cancer progression. CANCER SCI **2018**;109(7):2315-2326. https://doi.org/10.1111/cas.13629.
27. Huang L, Zhang L, Li T, Liu YW, Wang Y, Liu BJ. Human Plasma Metabolomics Implicates Modified 9-cis-Retinoic Acid in the Phenotype of Left Main Artery Lesions in Acute ST-Segment Elevated Myocardial Infarction. Sci Rep **2018**;8(1):12958. https://doi.org/10.1038/s41598-018-30219-w.
28. Wynn TA, Vannella KM. Macrophages in Tissue Repair, Regeneration, and Fibrosis. IMMUNITY **2016**;44(3):450-462. https://doi.org/10.1016/j.immuni.2016.02.015.
29. Lee S, Lim K. Phytoglycoprotein inhibits interleukin-1β and interleukin-6 via p38 mitogen-activated protein kinase in lipopolysaccharide-stimulated RAW 264.7 cells. Naunyn-Schmiedeberg's Archives of Pharmacology **2008**;377(1):45-54. https://doi.org/10.1007/s00210-007-0253-8.
30. Wu X, Zhao L, Peng H, She Y, Feng Y. Search for Potential Biomarkers by UPLC/Q-TOF–MS Analysis of Dynamic Changes of Glycerophospholipid Constituents of RAW264.7 Cells Treated With NSAID. CHROMATOGRAPHIA **2015**;78(3):211-220. https://doi.org/10.1007/s10337-014-2822-6.
31. Bordbar A, Mo ML, Nakayasu ES et al. Model-driven multi-omic data analysis elucidates metabolic immunomodulators of macrophage activation. MOL SYST BIOL **2012**;8:558. https://doi.org/10.1038/msb.2012.21.
32. Penkert RR, Jones BG, Häcker H, Partridge JF, Hurwitz JL. Vitamin A differentially regulates cytokine expression in respiratory epithelial and macrophage cell lines. CYTOKINE **2017**;91:1-5. https://doi.org/10.1016/j.cyto.2016.11.015.
33. de Oliveira MR, Da Rocha RF, Pasquali MADB, Moreira JCF. The effects of vitamin A supplementation for 3 months on adult rat nigrostriatal axis: Increased monoamine oxidase enzyme activity, mitochondrial redox dysfunction, increased β-amyloid1–40 peptide and TNF-α contents, and susceptibility of mitochondria to an in vitro H2O2 challenge. BRAIN RES BULL **2012**;87(4):432-444. https://doi.org/10.1016/j.brainresbull.2012.01.005.
34. Gasparotto J, Petiz LL, Girardi CS et al. Supplementation with vitamin A enhances oxidative stress in the lungs of rats submitted to aerobic exercise. Applied Physiology, Nutrition, and Metabolism **2015**;40(12):1253-1261. https://doi.org/10.1139/apnm-2015-0218.
35. Gelain DP, de Bittencourt Pasquali MA, Caregnato FF, Moreira JCF. Vitamin A (retinol) up-regulates the receptor for advanced glycation endproducts (RAGE) through p38 and Akt oxidant-dependent activation. TOXICOLOGY **2011**;289(1):38-44. https://doi.org/10.1016/j.tox.2011.07.008.

36. de Oliveira MR, Silvestrin RB, Mello E Souza T, Moreira JCF. Oxidative stress in the hippocampus, anxiety-like behavior and decreased locomotory and exploratory activity of adult rats: Effects of sub acute vitamin A supplementation at therapeutic doses. NEUROTOXICOLOGY **2007**;28(6):1191-1199. https://doi.org/10.1016/j.neuro.2007.07.008.
37. Pasquali MA, Gelain DP, Oliveira MR et al. Vitamin A supplementation induces oxidative stress and decreases the immunocontent of catalase and superoxide dismutase in rat lungs. EXP LUNG RES **2009**;35(5):427-438. https://doi.org/10.1080/01902140902747436.
38. Gelain DP, de Bittencourt Pasquali MA, Zanotto-Filho A et al. Retinol increases catalase activity and protein content by a reactive species-dependent mechanism in Sertoli cells. CHEM-BIOL INTERACT **2008**;174(1):38-43. https://doi.org/10.1016/j.cbi.2008.04.025.
39. Pasquali MAB, Gelain DP, Zanotto-Filho A et al. Retinol and retinoic acid modulate catalase activity in Sertoli cells by distinct and gene expression-independent mechanisms. TOXICOL IN VITRO **2008**;22(5):1177-1183. https://doi.org/10.1016/j.tiv.2008.03.007.
40. Gelain DP, Cammarota M, Zanotto-Filho A et al. Retinol induces the ERK1/2-dependent phosphorylation of CREB through a pathway involving the generation of reactive oxygen species in cultured Sertoli cells. CELL SIGNAL **2006**;18(10):1685-1694. https://doi.org/10.1016/j.cellsig.2006.01.008. https://doi.org/10.1016/j.cellsig.2006.01.008.
41. Zanotto-Filho A, Cammarota M, Gelain DP et al. Retinoic acid induces apoptosis by a non-classical mechanism of ERK1/2 activation. TOXICOL IN VITRO **2008**;22(5):1205-1212. https://doi.org/10.1016/j.tiv.2008.04.001.
42. Zanotto-Filho A, Gelain DP, Schröder R et al. The NFκB-mediated control of RS and JNK signaling in vitamin A-treated cells: Duration of JNK–AP-1 pathway activation may determine cell death or proliferation. BIOCHEM PHARMACOL **2009**;77(7):1291-1301. https://doi.org/10.1016/j.bcp.2008.12.010.
43. Fialkow L, Wang Y, Downey GP. Reactive oxygen and nitrogen species as signaling molecules regulating neutrophil function. FREE RADICAL BIO MED **2007**;42(2):153-164. https://doi.org/10.1016/j.freeradbiomed.2006.09.030.
44. Amiraslani B, Sabouni F, Abbasi S, Nazem H, Sabet M. Recognition of betaine as an inhibitor of lipopolysaccharide-induced nitric oxide production in activated microglial cells. Iranian biomedical journal **2012**;16(2):84-89. https://doi.org/10.6091/IBJ.1012.2012.
45. Nie C, Nie H, Zhao Y, Wu J, Zhang X. Betaine reverses the memory impairments in a chronic cerebral hypoperfusion rat model. NEUROSCI LETT **2016**;615:9-14. https://doi.org/10.1016/j.neulet.2015.11.019.
46. de Oliveira MR. Vitamin A and Retinoids as Mitochondrial Toxicants. OXID MED CELL LONGEV **2015**;2015:140267. https://doi.org/10.1155/2015/140267.
47. Baruteau J, Jameson E, Morris AA et al. Expanding the phenotype in argininosuccinic aciduria: need for new therapies. J INHERIT METAB DIS **2017**;40(3):357-368. https://doi.org/10.1007/s10545-017-0022-x.

48. Wang C, Chen H, Zhang M, Zhang J, Wei X, Ying W. Malate-aspartate shuttle inhibitor aminooxyacetic acid leads to decreased intracellular ATP levels and altered cell cycle of C6 glioma cells by inhibiting glycolysis. CANCER LETT **2016**;378(1):1-7. https://doi.org/10.1016/j.canlet.2016.05.001.
49. Gellerich FN, Gizatullina Z, Trumbekaite S et al. Cytosolic Ca²⁺ regulates the energization of isolated brain mitochondria by formation of pyruvate through the malate–aspartate shuttle. BIOCHEM J **2012**;443(3):747. https://doi.org/10.1042/BJ20110765.
50. Wang M, Xia W, Li H et al. Normal pregnancy induced glucose metabolic stress in a longitudinal cohort of healthy women: Novel insights generated from a urine metabolomics study. MEDICINE **2018**;97(40):e12417. https://doi.org/10.1097/MD.0000000000012417.
51. Kim D, Ko JM, Kim Y et al. Low prevalence of argininosuccinate lyase deficiency among inherited urea cycle disorders in Korea. J HUM GENET **2018**(4):1. https://doi.org/10.1038/s10038-018-0467-2.

Figures

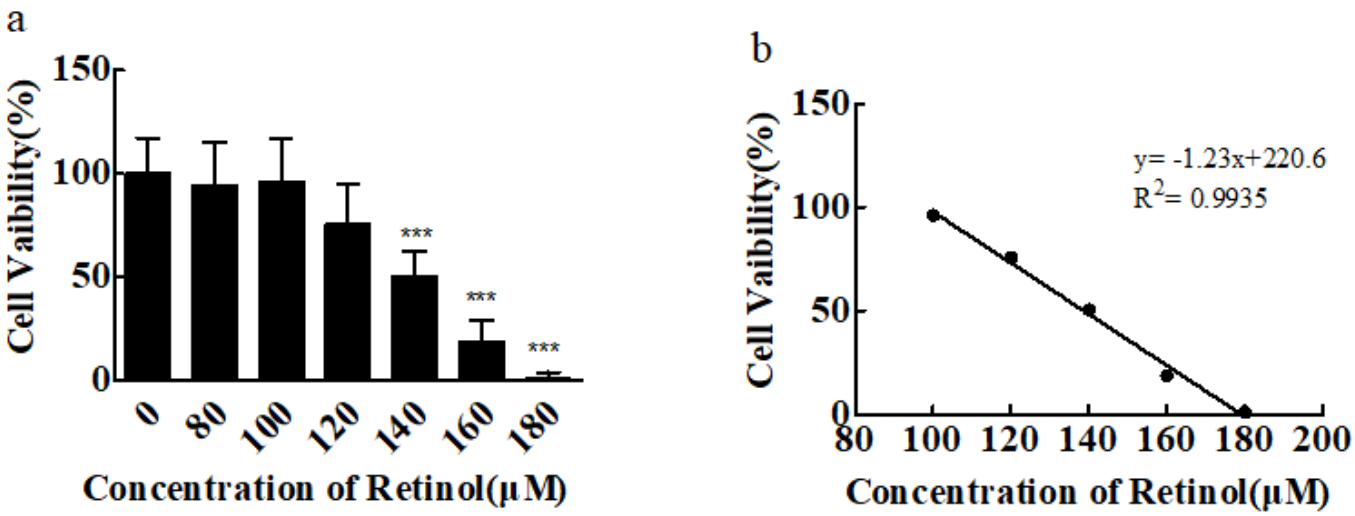

Figure 1

Effect of different concentrations of retinol(RET) on the survival rate of RAW264.7 cells (a) and linear regression equation (b). Note：***P<0.005 retinol group vs control group

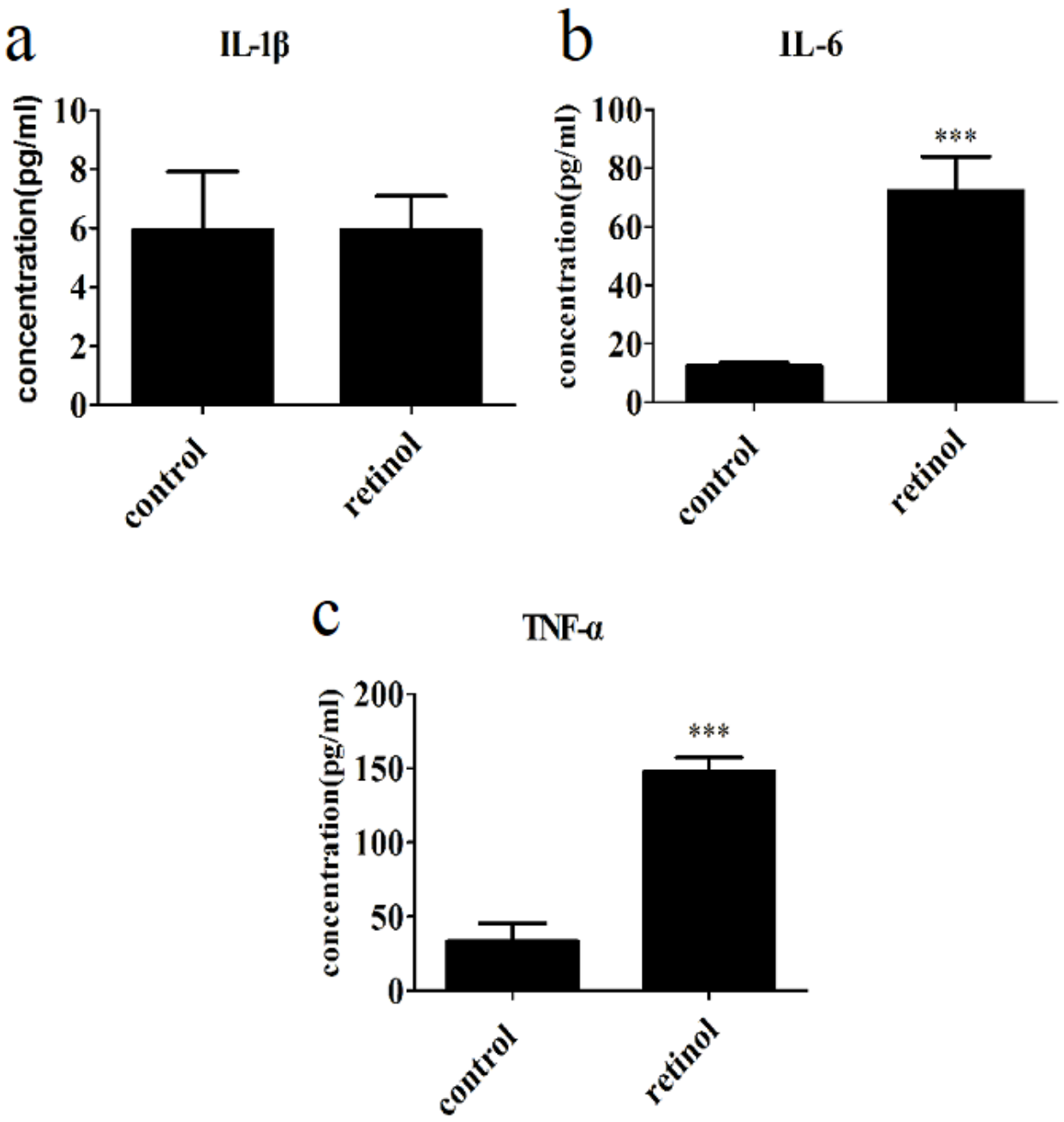

Figure 2

Effects of retinol on IL-1β (a), IL-6 (b) and TNF-α (c) in RAW264.7 cells(n=3) by ELISA. Note：***P<0.005 retinol group vs control group

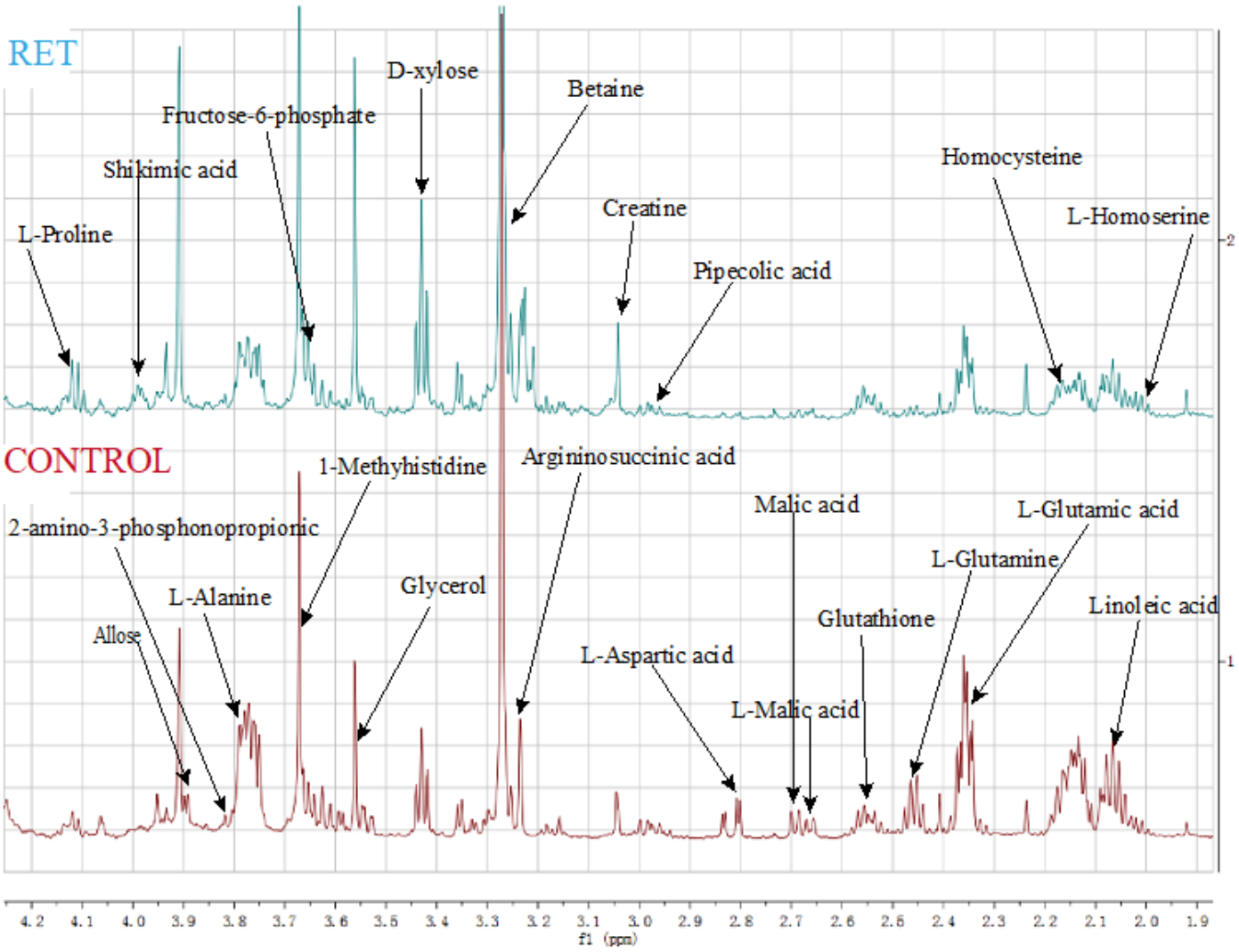

Figure 3

1H-NMR spectra of the retinol (RET) group and the control group of RAW 264.7 cells(n=6). Figure 4. Multivariate statistical analysis between the control group and the retinol treatment group. a. PCA score map; b. PLS-DA score map; c. OPLS-DA score map; d. The result of PLS-DA confidence test; e. The result of OPLS-DA confidence test.

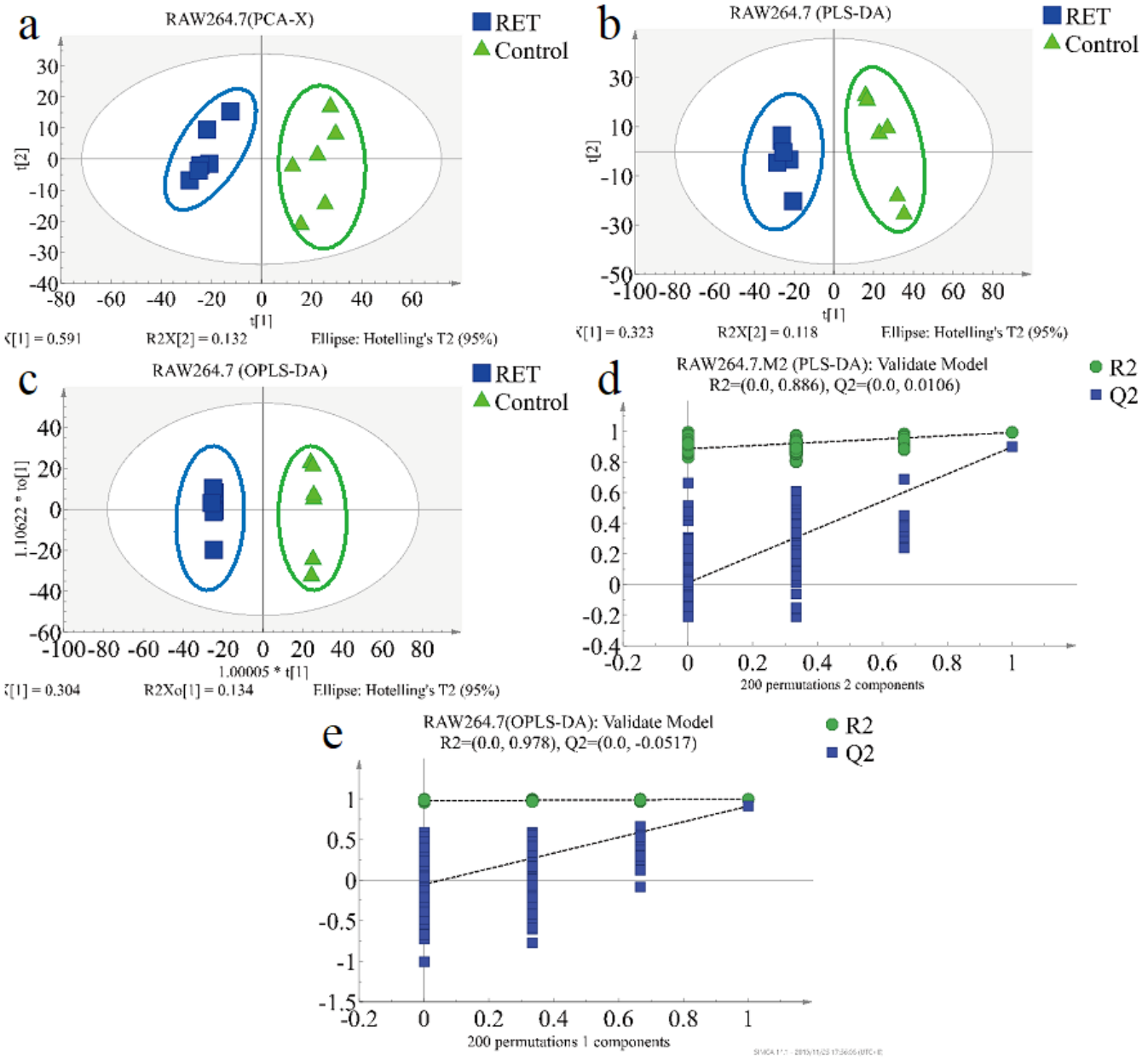

Figure 4

Multivariate statistical analysis between the control group and the retinol treatment group. a. PCA score map; b. PLS-DA score map; c. OPLS-DA score map; d. The result of PLS-DA confidence test; e. The result of OPLS-DA confidence test.

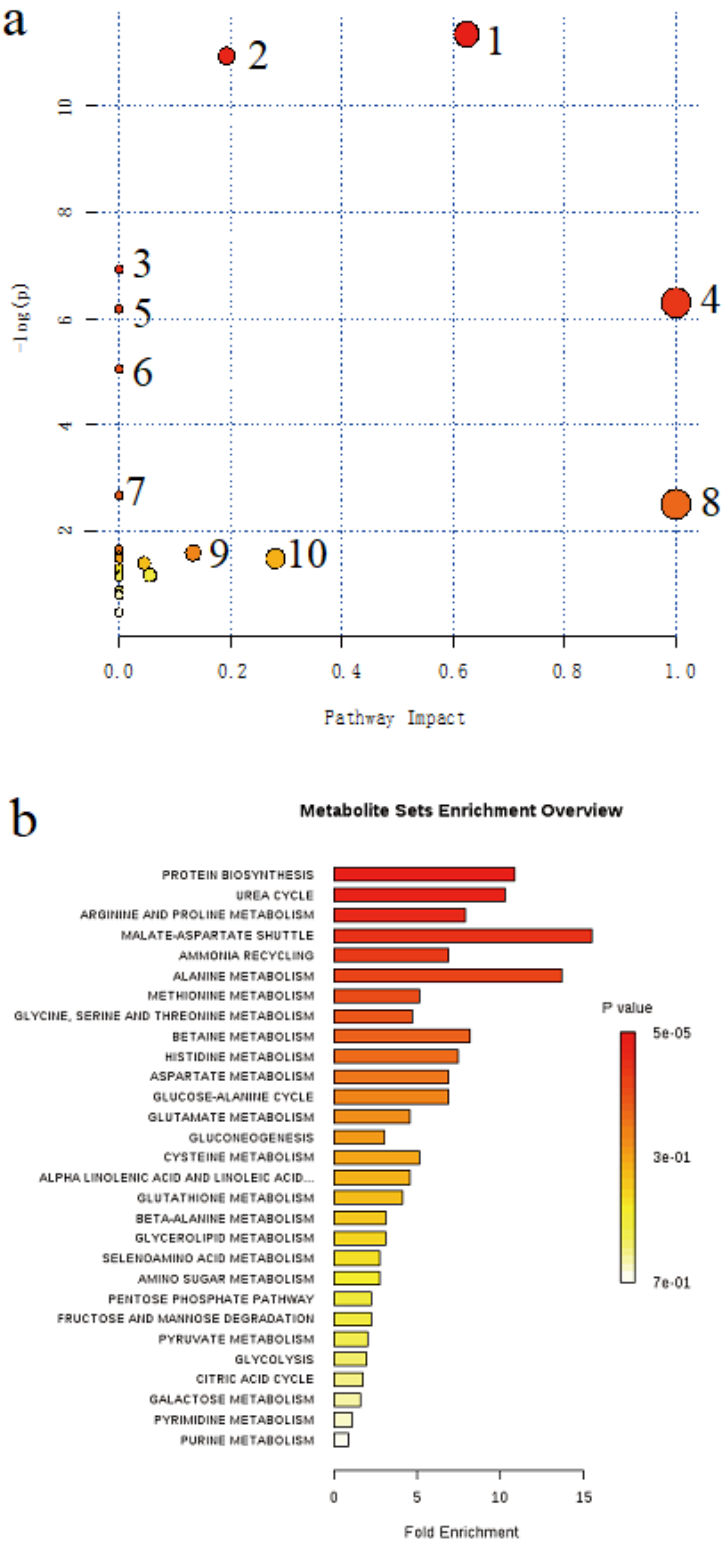

Figure 5

a. Metabolic pathways attributed to differential metabolites in RAW264.7 cells; b. Overview of metabolite enrichment in RAW264.7 cells. (1) alanine, aspartic acid and glutamate metabolism; (2) arginine and proline metabolism; (3) histidine metabolism; (4) D-Glutamine and D-glutamate metabolism (5) aminoacyl-tRNA biosynthesis; (6) nitrogen metabolism; (7) glycine, serine and threonine metabolism; (8) linoleic acid metabolism; (9) seleno amino acid metabolism; (10) Mutual conversion of sugar and

glucuronic acid. Note: The greater the -logP value of metabolic pathway effects, the higher the metabolic correlation between different groups.The larger the circle, the more red, and the more significant the signal path difference in the upper right corner.